HHS Public Access

Author manuscript

Med Biol Eng Comput. Author manuscript; available in PMC 2018 April 01.

Published in final edited form as:

Med Biol Eng Comput. 2017 April ; 55(4): 631–640. doi:10.1007/s11517-016-1544-3.

Assessing the mean strength and variations of the time-to-time fluctuations of resting-state brain activity

Zhengjun Li[1], **Yu-Feng Zang**[2,3], **Jianping Ding**[4], and **Ze Wang**[2,3,4]

[1]Department of Psychiatry, Perelman School of Medicine, University of Pennsylvania, 3900 Chestnut St, Philadelphia, PA 19104, USA

[2]Center for Cognition and Brain Disorders, Institutes of Neurological Science, Hangzhou Normal University, Hangzhou 310005, Zhejiang Province, China

[3]Zhejiang Key Laboratory for Research in Assessment of Cognitive Impairments, Hangzhou 310005, Zhejiang Province, China

[4]Affiliated Hospital, Hangzhou Normal University, 126 Wenzhou Rd, Building 7, MRI Room, Hangzhou 310015, Zhejiang Province, China

Abstract

The time-to-time fluctuations (TTFs) of resting-state brain activity as captured by resting-state fMRI (rsfMRI) have been repeatedly shown to be informative of functional brain structures and disease-related alterations. TTFs can be characterized by the mean and the range of successive difference. The former can be measured with the mean squared successive difference (MSSD), which is mathematically similar to standard deviation; the latter can be calculated by the variability of the successive difference (VSD). The purpose of this study was to evaluate both the resting state-MSSD and VSD of rsfMRI regarding their test–retest stability, sensitivity to brain state change, as well as their biological meanings. We hypothesized that MSSD and VSD are reliable in resting brain; both measures are sensitive to brain state changes such as eyes-open compared to eyes-closed condition; both are predictive of age. These hypotheses were tested with three rsfMRI datasets and proven true, suggesting both MSSD and VSD as reliable and useful tools for resting-state studies.

Keywords

Resting-state fMRI; Variation; Fluctuation

Correspondence to: Ze Wang.

Electronic supplementary material The online version of this article (doi:10.1007/s11517-016-1544-3) contains supplementary material, which is available to authorized users.

Compliance with ethical standards

Conflict of interest The authors declare that they have no conflict of interest.

Ethical approval All procedures performed in studies involving human participants were in accordance with the ethical standards of the institutional and/or national research committee and with the 1964 Helsinki Declaration and its later amendments or comparable ethical standards. For this type of retrospective study, formal consent is not required.

1 Introduction

The now overwhelming resting-state fMRI (rsfMRI)-based resting-state research starts from a scrutiny to the once assumed physiological “noise”: the restless fluctuations of brain activity at rest [5, 34]. Because the blood-oxygen-level-dependent (BOLD) signal generally acquired in rsfMRI is non-quantitative, a direct comparison of rsfMRI signal between different scan times or across subjects is meaningless. Rather, rsfMRI is assessed in relation to a reference region such as in the inter-regional functional connectivity (FC) analysis [5] or to the neighboring voxels or the baseline mean [27, 38, 40, 42, 44]. While these methods have been very successful for identifying consistent and informative resting-state brain activity patterns, they do not directly characterize the time-to-time fluctuations (TTFs) of brain activity at each voxel. Moreover, they usually only consider the slowly fluctuating components of rsfMRI, leaving the high-frequency part as “noise,” which certainly should be under scrutiny because fluctuations of neural activity, even if they look like high-frequency “noise,” have been found to beneficial for detecting weak signal [3, 13, 30, 41] or for achieving a large functional capacity for the neural system to respond to stimuli [25, 26, 36].

Two types of methods have been used to assess TTFs of resting-state brain activity using rsfMRI. The first one is to measure the power spectrum percentage of different frequency bands [32, 43, 45, 47]. Because the percentage is calculated in relation to the entire spectrum, these methods cannot provide a gross measure for the fluctuations of the entire temporal process. Another issue is that those methods need empirically determined frequency cutoffs to define different frequency bands, which may not be accurate and not suitable for assessing fluctuations with time-varying frequencies. The second type of methods directly characterizes TTFs by calculating statistical variability, such as variance or standard deviation (SD), two measures of the average disparity of the entire data samples to the mean value. These time-domain methods were widely used in biological signal processing [8, 19]. As compared to the frequency-based methods, the statistical approaches are independent of any a priori frequency band specifications and they provide an index for the extent of overall fluctuations. Fransson [15] first noticed that variance of BOLD fMRI decreased in the default mode network during task-induced deactivations. Samanez-Larkin et al. found that variability of BOLD fMRI measured by the mean squared successive difference (MSSD) [39] throughout the midbrain and striatum with peaks in the substantia nigra, ventral tegmental area increased with age when the subjects are performing a risk-taking task. Garrett et al. [16] calculated SD as a measure of regional variability of fMRI data during a resting (fixation) condition and found that a reduction in rsfMRI SD is predictive of aging. He [18] later noticed that variance of fMRI was higher during rest condition as compared to a task-performing condition. While these studies showed interesting findings about temporal brain fluctuations at rest, the resting-state data were extracted from the control resting blocks from task-performing experiments, which were inevitably affected by the task-performing blocks. Few studies have assessed TTFs of the brain using rsfMRI. Maxim et al. modeled the noise of rsfMRI data with a fractional Gaussian noise model and demonstrated that variance of rsfMRI was higher in ventricles and the rim of cortices and patients with Alzheimer’s disease had higher variance in places near

the ventricles and sulcal CSF [29]. Kaneoke et al. [21] showed higher variance also in regions near brain ventricles and CSF but lower variance in many other places including temporal lobes, striatum, insula, visual cortex, and prefrontal cortex. No one has yet paid attention to the higher-order TTFs.

The aims of this paper were to assess TTFs in the resting brain regarding its test–retest stability, sensitivity to state change, and associations with age. The former two remain new. The third part has been done in [16] but with a small cohort of subjects and not with rsfMRI. We used the large cohort from the 1000 Functional Connectomes Project (FCP) (http://fcon_1000.projects.nitrc.org). A fourth goal of this paper was to assess the second-order TTFs. While SD or variance of the raw rsfMRI data measures mean temporal fluctuations of the resting brain, they do not characterize second-order TTFs, which is the variation of the time-to-time fluctuation (mean change rate of the dynamic changes of the raw data, similar to the acceleration rate). The rationale for assessing the second-order TTFs is that if a range of dynamic neural activity (variability or the first-order TTFs) is required for the neural system to have an optimal performance in response to stimuli [25, 26, 36], it is likely that a range of the change rate of TTFs is also needed for the system to have a minimal time to respond to stimuli but still under some innate biological constraints such as energy and action potential magnitude and rate [2]. We assessed the mean strength and variation of the TTFs with the normalized MSSD (nMSSD), and the variability of successive difference (VSD), respectively. MSSD is a non-biased estimation to SD [39], but it involves a successive differentiation process which makes it less sensitive to low-frequency drift, a well-known confound in fMRI. Our hypotheses were: Both nMSSD and VSD of rsfMRI are stable across time; nMSSD and VSD can indicate brain activity changes such as eyes-open versus eyes-closed condition; nMSSD and VSD are predictive of age and are different across genders.

2 Method

2.1 Data and subjects

Three rsfMRI datasets were used for evaluating both nMSSD and VSD. Dataset 1 was acquired at the University of Pennsylvania; datasets 2 and 3 were downloaded from public neuroimaging sharing database.

Dataset 1 was reported in previous studies [22, 23, 40]. Sixteen young healthy human subjects [age 25 ± 4.6 (mean ± SD), age range 20–35, 7 males] were recruited from local community in Philadelphia. The study was approved by the University of Pennsylvania Institutional Review Board, and all subjects provided signed written consent form before being enrolled in the experiments. All subjects' information was anonymized and de-identified prior to analysis in this study.

Dataset 2 was provided by Zang et al. from Beijing Normal University [28]. Forty-eight subjects (age: 22.5 ± 2.2, age range 18–30, 24 males) were scanned twice; one session with eyes open and the other with eyes closed (EOEC). Imaging data were downloaded from http://fcon_1000.projects.nitrc.org/indi/IndiPro.html [28].

Dataset 3 was also downloaded from the 1000 Functional Connectomes Project (FCP) Web site (http://fcon_1000.projects.nitrc.org). One thousand and forty-nine subjects from 22 different sites were included as in our previous paper [40] (age = 26.94 ± 11.34) years, age range: 7.88–85 years, 466 males, 583 females).

The collection and publicly sharing of datasets 2 and 3 were approved by each contributor's respective ethics committee. See Refs. [28] and [6] for details. All subjects' imaging data were anonymized and de-identified prior to download and analysis.

2.2 Imaging acquisition

For dataset 1, all MR images were acquired on a Siemens 3 Tesla Trio whole-body scanner (Erlangen, Germany) at the Hospital of the University of Pennsylvania using an eight-channel array coil. High-resolution T1-weighted images were acquired using a 3D-MPRAGE sequence with following parameters: TR = 1620 ms, TE = 3 ms, flip angle = 15°, and slice thickness = 1.0 mm. Resting-state fMRI images were acquired using a T2*-weighted gradient echo echo-planar-imaging (EPI) sequence with following parameters: TR = 2 s, TE = 30 ms, slice thickness = 3.3 mm, 35 slices, FOV = 220 × 220 mm^2, matrix = 64 × 64, and 150 time points. During the resting-state scan, the subjects were instructed to lie still and keep eyes open [22, 23]. Each subject took a second (retest) scan about 2 months after the first scan.

The EOEC data (dataset 2) were acquired in a Siemens Trio 3T whole-body scanner too. Each subject underwent one high-resolution T1 3D-MPRAGE scan: TR = 2530 ms, TE = 3.39 ms, flip angle = 7°, and slice thickness = 1.33 mm, and 3 resting-state fMRI scans with the following parameters: TR = 2 s, TE = 30 ms, slice thickness = 3.5 mm, slice gap = 0.7 m, 33 slices, FOV = 200 × 200 mm^2, matrix = 64 × 64, and 240 time points [28]. The second and third resting-state scans were shuffled and counterbalanced across the subjects so that half of the subjects were instructed to close their eyes during the second scan and instructed to keep their eyes open during the third scan, and the other half of the subjects were instructed to keep their eyes open during the second scan and keep their eyes closed during the third scan [28]. These two EOEC scans were used in this study.

Acquisition parameters for the rsfMRI dataset 3 were: imaging duration: 4.15–9.8 min; voxel size: 2–4 mm within plane; and slice thickness, 3–5.5 mm. Structural images were acquired as well. Full acquisition settings can be found in the 1000 FCP webpage http://fcon_1000.projects.nitrc.org.

2.3 Data preprocessing

Data preprocessing was performed with the standard pipeline [6] using FSL [20] and AFNI [11] software. Briefly, the rsfMRI images were corrected for slice timing and motion, and were subsequently smoothed using a Gaussian kernel with full width at half maximum (FWHM) = 6 mm [31] and high-pass filtered (0.009 Hz). CSF and white matter signals, as well as the motion parameters and their derivatives, were regressed out.

2.4 Metrics of TTF

The mean strength and variation of rsfMRI TTF with respect to time were calculated as the nMSSD and the VSD. Since fMRI is a relative measure, we removed the scale by dividing the TTF metrics by the mean of rsfMRI signal at each voxel. Assuming that rsfMRI time series at one voxel is $[x_1, x_2, \ldots, x_n]$ (n is the number of acquisitions), its first derivative with respect to time was calculated as $dx = [dx_1, dx_2, \ldots, dx_{n-1}]$, where $dx_j = x_{j+1} - x_j$. Then, the nMSSD was calculated by

$$\mathrm{nMSSD}(x)=\frac{\mathrm{sqrt}(1/(n-1)\sum_{j=1}^{n-1}(\mathrm{d}x_j)^2)}{(1/n\sum_{j=1}^{n}x_j)} \quad (1)$$

VSD was calculated as

$$\mathrm{VSD}(x)=\frac{\mathrm{SD}(|\mathrm{d}x|)}{1/n\sum_{j=1}^{n}x_j} \quad (2)$$

where SD means taking standard deviation and |.| means taking absolute. To avoid digital data underflow during processing, nMSSD and VSD were multiplied by 1000, respectively. nMSSD and VSD maps were smoothed and registered into the Montreal Neurological Institute (MNI) standard brain space using FSL FNIRT.

2.5 Group-level analysis

Test–retest reliability was evaluated with intra-class correlation (ICC) [37]. First, one-way ANOVA was used to calculate the within-subject mean square (MS_w) and between-subject mean square (MS_b). ICC value was then calculated according to the following equation voxel by voxel [37].

$$\mathrm{ICC}=\frac{\mathrm{MS_b}-\mathrm{MS_w}}{\mathrm{MS_b}+(k-1)\mathrm{MS_w}} \quad (3)$$

where $K = 2$ is the number of observations for each subject. ICC value ranges from 0.0 to 1.0. Cicchetti et al. [9, 10] proposed a guideline to quantify the reliability as poor (ICC below 0.4), fair (ICC in the range of 0.41–0.59), good (ICC in the range of 0.60–0.74), or excellent (ICC above 0.75). Portney et al. [33] suggested that an ICC < 0.5 represents poor reliability, ICC in the range of 0.5–0.74 represents moderate reliability, and ICC > 0.75 represents good reliability. Therefore, an ICC > 0.5 is often chosen as an acceptable reliability criteria in many studies [1, 22, 35], and was used in this paper to define high test–retest stability too.

Paired *T* test was performed to assess the nMSSD and VSD difference between the EO and EC resting state using the EOEC dataset. The statistical significance was defined with an uncorrected *p* value of 0.001 and a spatial extent threshold of 30 voxels [24] [4].

The 1049 FCP data were used to test the hypothesis that nMSSD and VSD are predictive of age and gender. TR (the sampling rate of rsfMRI) was divided off from both nMSSD and VSD to convert them into sampling rate-independent values. Simple regression was used to assess the relation of each voxel's nMSSD or VSD to age or gender (both in the same model). Because the sample size of the FCP data is large, a family-wise error (FWE)-corrected p value of 0.05 was used to define the significant relationship clusters.

3 Results

3.1 Mean nMSSD and VSD map

To give an intuitive view of nMSSD and VSD of the TTF in the resting brain, Fig. 1 shows the averaged nMSSD (calculated with Eq. 1) and the averaged VSD (calculated with Eq. 2) of the test–retest rsfMRI scans of the young healthy subjects from dataset 1. The mean nMSSD of the first scans of the young subjects (Fig. 1a) was very similar to the mean nMSSD of the second (retest) scans (Fig. 1b). The mean VSD of the first scans of the young subjects (Fig. 1c) was also very similar to the mean VSD of the second scans (Fig. 1d). Both nMSSD and VSD of brain tissue regions were lower than those of CSF regions.

To test the difference between nMSSD and VSD, we presented the ratio of nMSSD and VSD of one scan of one example subject in Fig. 1e. In Fig. 1e, each voxel showed the value of nMSSD of that location divided by VSD of the same location. In this figure, similar but not the same nMSSD/VSD ratios were shown across the brain.

3.2 Test–retest reliability of nMSSD and VSD

Figure 2 shows the test–retest stability analysis results. Both nMSSD (Fig. 2a) and VSD (Fig. 2b) showed very high ICC scores (calculated with Eq. 3) in nearly the entire gray matter, especially in visual cortex, posterior cingulate cortex, precuneus, parietal cortex, and frontal lobe. nMSSD and VSD showed very similar spatial distribution patterns of ICC scores across the brain though VSD showed spatially more extended high ICC (>0.5) distributions.

3.3 Resting nMSSD and VSD changes in response to the EO–EC state change

Figure 3 shows the EO–EC state change-induced TTF alterations. As compared to the eyes-closed condition, the eyes-open resting condition had lower nMSSD (Fig. 3a) and lower VSD (Fig. 3b) in superior temporal cortex, middle temporal cortex, visual cortex, basal ganglia, and the motor network including primary cortex, supplementary motor area (SMA), and thalamus. Eyes-open condition showed higher VSD (Fig. 3b) in bilateral middle occipital lobe. The hypo (lower in the eyes-open condition) patterns of nMSSD and VSD appeared to be similar, but VSD presented larger and more spatially distributed supra-threshold clusters. While the results were presented with an uncorrected threshold similar to the previous EO–EC papers, a portion of the EO–EC nMSSD and VSD difference patterns

sustained even with a more stringent threshold ($p < 0.05$, FWE corrected) as shown in Supplementary Fig S2.

3.4 Age and gender effects of rsfMRI nMSSD and VSD

Figure 4 shows the regression analysis results from the 1049 FCP dataset. nMSSD was negatively ($p < 0.05$ with family-wise error (FWE) correction) correlated with age in visual cortex, posterior cingulate cortex (PCC), precuneus, bilateral parietal cortex, and right dorsolateral prefrontal cortex (dlPFC) (Fig. 4a). VSD showed negative correlation (Fig. 4c) with age in similar regions. In addition, VSD showed correlation with age in left lateral orbito-frontal cortex (OFC). No positive correlations were found between age and nMSSD or VSD. As compared to females, male subjects had higher nMSSD (Fig. 4b) and VSD (Fig. 4d) in frontal lobe, caudate, insula, temporal cortex, anterior cingulate cortex (ACC), and cerebellum. VSD was higher in males in the same regions with larger cluster extension. Additional supra-threshold clusters of higher male VSD was found in ventral striatum and hippocampus.

4 Discussion

In this study, we characterized the time-to-time fluctuations in the resting brain using rsfMRI acquired without any task-performing interference. We assessed both the mean and the range of the time-to-time rsfMRI changes using nMSSD and VSD. nMSSD provides a scale-free measure for the mean squared differentiations of the raw rsfMRI and can be considered as a mean time-to-time fluctuation index. VSD characterizes the relative (or scale-free) standard deviation of the time-to-time rsfMRI signal changes and can be considered as a second-order variability measure. If normalized by the time of repetition (TR, the sampling rate of rsfMRI), nMSSD and VSD are similar to the mean speed and acceleration of the dynamic resting-state activity, respectively, which are both related to kinetic energy. Because human brain is an energy-constrained system [14] and consistent brain functionality needs a consistent energy consumption, it is likely that resting brain presents spatially distributed nMSSD and VSD and both measures would be stable across time. Although TTFs have been recently studied with standard deviation and MSSD, their patterns in resting brain remained unclear, not to mention their test–retest stability. This paper aimed to address these unsolved issues.

Using test–retest rsfMRI, we showed high reproducibility of both measures in most of the cerebral cortex. Gray matter had higher nMSSD and VSD than white matter because of more neural activity going on in gray matter. CSF shows the highest nMSSD and VSD because BOLD fMRI signal in CSF is mainly contributed by random noise. The test–retest analysis results and the inhomogeneous nMSSD/VSD ratio shown in this paper suggest nMSSD and VSD as two different but reliable indices for characterizing resting-state brain activity. Using rsfMRI data acquired with eyes closed and eyes open, nMSSD and VSD revealed brain difference patterns similar to those reported in previous studies [28, 46], suggesting that nMSSD and VSD are sensitive to regional activity alterations during brain state change.

To examine the neurobiological relationship of nMSSD and VSD, we calculated their correlations with age and gender using a large cohort of subjects (n = 1049). The results repeated previously observed negative correlations between rsfMRI variability and age in visual cortex, precuneus, bilateral parietal cortex, lateral inferior frontal cortex, bilateral dlPFC, and PFC [16]. Precuneus, bilateral parietal cortex are parts of the default mode network whose resting activity has been shown to decrease with age by Damoiseaux et al. [12] early in 2008. VSD showed similar negative correlations with age. Different from [16], we did not find any positive correlations between resting TTFs and age. The main reason for this discrepancy could be the larger sample size and the more strict multiple comparison correction method used in this paper. Biswal et al. [6] reported both positive and negative correlations between age and ALFF. The negative correlations were located in similar areas to what we found in nMSSD or VSD but were more spatially distributed. Two reasons can contribute to such a difference. First, standard ALFF analysis only considers one particular frequency band but nMSSD and VSD are not constrained to any frequency bands. Second, a cluster-wise multiple comparison correction method was used in [6] which is different from the voxel-wise Bonferroni correction approach. Nevertheless, the decreased nMSSD and VSD in aging brain are consistent with previous studies based on variability and ALFF and suggest a less active and less adaptable resting state in the older adults. We observed a widespread gender effect in both nMSSD and VSD with males showing higher nMSSD and VSD, which is opposed to the higher ALFF in females' findings in [6]. As mentioned above, nMSSD and VSD are independent of any specific frequency band, so they can be very different from what ALFF measures. Nevertheless, the higher nMSSD and VSD in males may be related to a higher energy consumption level in males' brain as compared to females.

VSD seems to be relatively more sensitive for detecting the EOEC effects, for predicting age as well as gender. Theoretically, VSD is related to acceleration which is more directly related to kinetic energy than nMSSD. Since energy is the base of neural activity, the relatively higher sensitivity of VSD may suggest that VSD better reflects neural activity than nMSSD.

Default mode network has been repeatedly shown to have higher low-frequency fluctuations than the rest of the brain during rest [7, 34]. Such a contrast, however, was not clear in the resting nMSSD and VSD map in this paper. One reason could be that both nMSSD and VSD quantify TTF of the full spectrum rather than the low-frequency partition. Higher low-frequency TTF in DMN does not necessarily mean higher TTF in the entire frequency band in DMN. Second, the traditional resting-state fMRI measures such as functional connectivity and amplitude of low-frequency fluctuations, are based on the original time series, but nMSSD and VSD are based on the absolute successive difference, which is different from the original time series and may contribute to the observed spatial distribution pattern difference.

The sampling rate (TR of rsfMRI) may affect both nMSSD and VSD. But as long as the same TR is used for all scans, its effects on the group-level comparison will be canceled out. We did control TR in the age and gender effects analysis because different TRs were used for the FCP data. But we noticed quite similar effects even without controlling TR.

In rsfMRI, noise from human physiological motion is an unresolved problem, and head motion differences between groups may induce spurious group difference of rsfMRI metrics [17]. In current study, there was no significant difference of head motion between the compared groups: The mean relative head displacement of the two test–rest sessions of young healthy dataset was 0.047 ± 0.024 and 0.041 ± 0.016 mm ($p = 0.345$); the mean relative head displacement of the EO and EC sessions of Beijing EC–EC dataset was 0.042 ± 0.015 and 0.046 ± 0.019 mm ($p = 0.057$), respectively [20]. In addition to rigid head motion correction, we also regressed out the first derivatives of all the nuisance signals (6 motion parameters and CSF, white matter signals) during image preprocessing, which should have substantially reduced the artifact induced by in-scanner subject physiological motion.

5 Conclusions

In summary, we found very high test–retest reliability of both nMSSD and VSD of rsfMRI in nearly the entire brain cortex, suggesting that the two TTF metrics are reproducible across time. We observed significant changes of nMSSD and VSD between the EO–EC sessions, indicating their sensitivity to brain state change. We also detected significant correlation between the two metrics and the age. These findings suggest nMSSD and VSD as reproducible and sensitive measures of brain dynamic fluctuations. Future studies are needed to assess their usefulness in translational applications and validate them as potential clinical biomarkers.

Supplementary Material

Refer to Web version on PubMed Central for supplementary material.

Acknowledgments

This study was supported by the Hangzhou Qianjiang Endowed Professor Program, the Youth 1000 Talent Program of China, Natural Science Foundation of Zhejiang Province Grant LZ15H180001, and NIH Grant 1R56DA036556. Data acquisition for dataset 3 was supported by National Natural Science Foundation of China Grant 30770594 and the National High Technology Program of China (863) Grant 2008AA02Z405.

References

1. Aron AR, Gluck MA, Poldrack RA. Long-term test-retest reliability of functional MRI in a classification learning task. Neuroimage. 2006; 29:1000–1006. DOI: 10.1016/j.neuroimage.2005.08.010 [PubMed: 16139527]
2. Attwell D, Laughlin SB. An energy budget for signaling in the grey matter of the brain. J Cereb Blood Flow Metab. 2001; 21:1133–1145. DOI: 10.1097/00004647-200110000-00001 [PubMed: 11598490]
3. Basalyga G, Salinas E. When response variability increases neural network robustness to synaptic noise. Neural Comput. 2006; 18:1349–1379. DOI: 10.1162/neco.2006.18.6.1349 [PubMed: 16764507]
4. Bennett CM, Wolford GL, Miller MB. The principled control of false positives in neuroimaging. Soc Cogn Affect Neurosci. 2009; 4:417–422. DOI: 10.1093/scan/nsp053 [PubMed: 20042432]
5. Biswal B, Yetkin FZ, Haughton VM, Hyde JS. Functional connectivity in the motor cortex of resting human brain using echo-planar mri. Magn Reson Med. 1995; 34:537–541. DOI: 10.1002/mrm.1910340409 [PubMed: 8524021]

6. Biswal BB, Mennes M, Zuo XN, Gohel S, Kelly C, Smith SM, Beckmann CF, Adelstein JS, Buckner RL, Colcombe S, Dogonowski AM, Ernst M, Fair D, Hampson M, Hoptman MJ, Hyde JS, Kiviniemi VJ, Kotter R, Li SJ, Lin CP, Lowe MJ, Mackay C, Madden DJ, Madsen KH, Margulies DS, Mayberg HS, McMahon K, Monk CS, Mostofsky SH, Nagel BJ, Pekar JJ, Peltier SJ, Petersen SE, Riedl V, Rombouts SA, Rypma B, Schlaggar BL, Schmidt S, Seidler RD, Siegle GJ, Sorg C, Teng GJ, Veijola J, Villringer A, Walter M, Wang L, Weng XC, Whitfield-Gabrieli S, Williamson P, Windischberger C, Zang YF, Zhang HY, Castellanos FX, Milham MP. Toward discovery science of human brain function. Proc Natl Acad Sci USA. 2010; 107:4734–4739. DOI: 10.1073/pnas.0911855107 [PubMed: 20176931]
7. Buckner RL, Andrews-Hanna JR, Schacter DL. The brain's default network: anatomy, function, and relevance to disease. Ann N Y Acad Sci. 2008; 1124:1–38. DOI: 10.1196/annals.1440.011 [PubMed: 18400922]
8. Challis RE, Kitney RI. Biomedical signal processing (in four parts). Part 1. Time-domain methods. Med Biol Eng Comput. 1990; 28:509–524. [PubMed: 2287173]
9. Cicchetti DV. The precision of reliability and validity estimates re-visited: distinguishing between clinical and statistical significance of sample size requirements. J Clin Exp Neuropsychol. 2001; 23:695–700. DOI: 10.1076/jcen.23.5.695.1249 [PubMed: 11778646]
10. Cicchetti DV, Sparrow SA. Developing criteria for establishing interrater reliability of specific items: applications to assessment of adaptive behavior. Am J Ment Defic. 1981; 86:127–137. [PubMed: 7315877]
11. Cox RW. AFNI: what a long strange trip it's been. Neuroimage. 2012; 62:743–747. DOI: 10.1016/j.neuroimage.2011.08.056 [PubMed: 21889996]
12. Damoiseaux JS, Beckmann CF, Arigita EJ, Barkhof F, Scheltens P, Stam CJ, Smith SM, Rombouts SA. Reduced resting-state brain activity in the "default network" in normal aging. Cereb Cortex. 2008; 18:1856–1864. DOI: 10.1093/cercor/bhm207 [PubMed: 18063564]
13. Faisal AA, Selen LPJ, Wolpert DM. Noise in the nervous system. Nat Rev Neurosci. 2008; 9:292–303. DOI: 10.1038/Nrn2258 [PubMed: 18319728]
14. Fonseca-Azevedo K, Herculano-Houzel S. Metabolic constraint imposes tradeoff between body size and number of brain neurons in human evolution. Proc Natl Acad Sci USA. 2012; 109:18571–18576. DOI: 10.1073/pnas.1206390109 [PubMed: 23090991]
15. Fransson P. Spontaneous low-frequency BOLD signal fluctuations: an fMRI investigation of the resting-state default mode of brain function hypothesis. Hum Brain Mapp. 2005; 26:15–29. DOI: 10.1002/hbm.20113 [PubMed: 15852468]
16. Garrett DD, Kovacevic N, McIntosh AR, Grady CL. Blood oxygen level-dependent signal variability is more than just noise. J Neurosci. 2010; 30:4914–4921. DOI: 10.1523/Jneurosci.5166-09.2010 [PubMed: 20371811]
17. Goto M, Abe O, Miyati T, Yamasue H, Gomi T, Takeda T. Head motion and correction methods in resting-state functional MRI. Magn Reson Med Sci. 2015; doi: 10.2463/mrms.rev.2015-0060
18. He BJ. Scale-free properties of the functional magnetic resonance imaging signal during rest and task. J Neurosci. 2011; 31:13786–13795. DOI: 10.1523/JNEUROSCI.2111-11.2011 [PubMed: 21957241]
19. Huang HH, Lee YH, Chan HL, Wang YP, Huang CH, Fan SZ. Using a short-term parameter of heart rate variability to distinguish awake from isoflurane anesthetic states. Med Biol Eng Comput. 2008; 46:977–984. DOI: 10.1007/s11517-008-0342-y [PubMed: 18414913]
20. Jenkinson M, Beckmann CF, Behrens TE, Woolrich MW, Smith SM. FSL. Neuroimage. 2012; 62:782–790. DOI: 10.1016/j.neuroimage.2011.09.015 [PubMed: 21979382]
21. Kaneoke Y, Donishi T, Iwatani J, Ukai S, Shinosaki K, Terada M. Variance and autocorrelation of the spontaneous slow brain activity. PLoS One. 2012; 7:e38131.doi: 10.1371/journal.pone.0038131 [PubMed: 22666461]
22. Li Z, Kadivar A, Pluta J, Dunlop J, Wang Z. Test-retest stability analysis of resting brain activity revealed by blood oxygen level-dependent functional MRI. J Magn Reson Imaging. 2012; 36:344–354. DOI: 10.1002/jmri.23670 [PubMed: 22535702]

23. Li Z, Zhu Y, Childress AR, Detre JA, Wang Z. Relations between BOLD fMRI-derived resting brain activity and cerebral blood flow. PLoS One. 2012; 7:e44556.doi: 10.1371/journal.pone.0044556 [PubMed: 23028560]
24. Lieberman MD, Cunningham WA. Type I and type II error concerns in fMRI research: re-balancing the scale. Soc Cogn Affect Neurosci. 2009; 4:423–428. DOI: 10.1093/scan/nsp052 [PubMed: 20035017]
25. Lipsitz LA. Physiological complexity, aging, and the path to frailty. Sci Aging Knowl Environ SAGE KE 2004. 2004; :pe16.doi: 10.1126/sageke.2004.16.pe16
26. Lipsitz LA, Goldberger AL. Loss of complexity and aging—potential applications of fractals and chaos theory to senescence. JAMA. 1992; 267:1806–1809. DOI: 10.1001/jama.1992.03480130122036 [PubMed: 1482430]
27. Liu CY, Krishnan AP, Yan L, Smith RX, Kilroy E, Alger JR, Ringman JM, Wang DJ. Complexity and synchronicity of resting state blood oxygenation level-dependent (BOLD) functional MRI in normal aging and cognitive decline. J Magn Reson Imaging. 2013; 38:36–45. DOI: 10.1002/jmri.23961 [PubMed: 23225622]
28. Liu D, Dong Z, Zuo X, Wang J, Zang Y. Eyes-open/eyes-closed dataset sharing for reproducibility evaluation of resting state fMRI data analysis methods. Neuroinformatics. 2013; 11:469–476. DOI: 10.1007/s12021-013-9187-0 [PubMed: 23836389]
29. Maxim V, Sendur L, Fadili J, Suckling J, Gould R, Howard R, Bullmore E. Fractional Gaussian noise, functional MRI and Alzheimer's disease. NeuroImage. 2005; 25:141–158. DOI: 10.1016/j.neuroimage.2004.10.044 [PubMed: 15734351]
30. McDonnell MD, Ward LM. The benefits of noise in neural systems: bridging theory and experiment. Nat Rev Neurosci. 2011; 12:U415–U489. DOI: 10.1038/Nrn3061
31. Mikl M, Marecek R, Hlustik P, Pavlicova M, Drastich A, Chlebus P, Brazdil M, Krupa P. Effects of spatial smoothing on fMRI group inferences. Magn Reson Imaging. 2008; 26:490–503. DOI: 10.1016/j.mri.2007.08.006 [PubMed: 18060720]
32. Niazy RK, Xie J, Miller K, Beckmann CF, Smith SM. Spectral characteristics of resting state networks. Prog Brain Res. 2011; 193:259–276. DOI: 10.1016/B978-0-444-53839-0.00017-X [PubMed: 21854968]
33. Portney, LG., Watkins, MP. Foundations of clinical research: applications to practice. Vol. 2. Prentice Hall; Upper Saddle River: 2000.
34. Raichle ME, MacLeod AM, Snyder AZ, Powers WJ, Gusnard DA, Shulman GL. A default mode of brain function. PNAS. 2001; 98:676–682. DOI: 10.1073/pnas.98.2.676 [PubMed: 11209064]
35. Shehzad Z, Kelly AMC, Reiss PT, Gee DG, Gotimer K, Uddin LQ, Lee SH, Margulies DS, Roy AK, Biswal BB, Petkova E, Castellanos FX, Milham MP. The resting brain: unconstrained yet reliable. Cereb Cortex. 2009; 19:2209–2229. DOI: 10.1093/cercor/bhn256 [PubMed: 19221144]
36. Shew WL, Yang H, Yu S, Roy R, Plenz D. Information capacity and transmission are maximized in balanced cortical networks with neuronal avalanches. Journal Neurosci. 2011; 31:55–63. DOI: 10.1523/JNEUROSCI.4637-10.2011
37. Shrout P, Fleiss J. Intraclass correlations: uses in assessing rater reliability. Psychol Bull. 1979; 86:420–428. [PubMed: 18839484]
38. Sokunbi MO, Staff RT, Waiter GD, Ahearn TS, Fox HC, Deary IJ, Starr JM, Whalley LJ, Murray AD. Inter-individual differences in fMRI entropy measurements in old age. IEEE Trans Biomed Eng. 2011; 58:3206–3214. DOI: 10.1109/TBME.2011.2164793 [PubMed: 21859598]
39. von Neumann J, Bellinson HR, Hart BI. The mean square successive difference. Ann Math Stat. 1941; 12:153–162.
40. Wang Z, Li Y, Childress AR, Detre JA. Brain entropy mapping using fMRI. PLoS One. 2014; 9:e89948.doi: 10.1371/journal.pone.0089948 [PubMed: 24657999]
41. Wilke SD, Eurich CW. On the functional role of noise correlations in the nervous system. Neurocomputing. 2002; 44:1023–1028. DOI: 10.1016/S0925-2312(02)00506-4
42. Yang AC, Huang CC, Yeh HL, Liu ME, Hong CJ, Tu PC, Chen JF, Huang NE, Peng CK, Lin CP, Tsai SJ. Complexity of spontaneous BOLD activity in default mode network is correlated with cognitive function in normal male elderly: a multiscale entropy analysis. Neurobiol Aging. 2013; 34:428–438. DOI: 10.1016/j.neurobiolaging.2012.05.004 [PubMed: 22683008]

43. Yuan BK, Wang J, Zang YF, Liu DQ. Amplitude differences in high-frequency fMRI signals between eyes open and eyes closed resting states. Front Hum Neurosci. 2014; 8:503.doi: 10.3389/fnhum.2014.00503 [PubMed: 25071530]

44. Zang Y, Jiang T, Lu Y, He Y, Tian L. Regional homogeneity approach to fMRI data analysis. Neuroimage. 2004; 22:394–400. DOI: 10.1016/j.neuroimage.2003.12.030 [PubMed: 15110032]

45. Zang YF, He Y, Zhu CZ, Cao QJ, Sui MQ, Liang M, Tian LX, Jiang TZ, Wang YF. Altered baseline brain activity in children with ADHD revealed by resting-state functional MRI. Brain Dev. 2007; 29:83–91. DOI: 10.1016/j.braindev.2006.07.002 [PubMed: 16919409]

46. Zou QH, Yuan BK, Gu H, Liu DQ, Wang DJJ, Gao JH, Yang YH, Zang YF. Detecting static and dynamic differences between eyes-closed and eyes-open resting states using ASL and BOLD fMRI. PLoS One. 2015; doi: 10.1371/journal.pone.0121757

47. Zuo XN, Di Martino A, Kelly C, Shehzad ZE, Gee DG, Klein DF, Castellanos FX, Biswal BB, Milham MP. The oscillating brain: complex and reliable. NeuroImage. 2010; 49:1432–1445. DOI: 10.1016/j.neuroimage.2009.09.037 [PubMed: 19782143]

Biographies

Zhengjun Li, Ph.D., is a biomedical engineer with extensive specialty in resting-state fMRI (rsfMRI) and arterial spin labeling (ASL) perfusion MRI signal processing.

Yu-Feng Zang, M.D., mainly focuses on rsfMRI research. He has developed several widely used tools for rsfMRI analysis.

Jianping Ding, M.D., is a radiologist. He has been performing MRI-based research for many years.

Ze Wang, Ph.D., major research directions include arterial spin labeling perfusion MRI, fMRI signal processing, and imaging-based addiction research. He has developed various algorithms and tools for ASL MRI and fMRI.

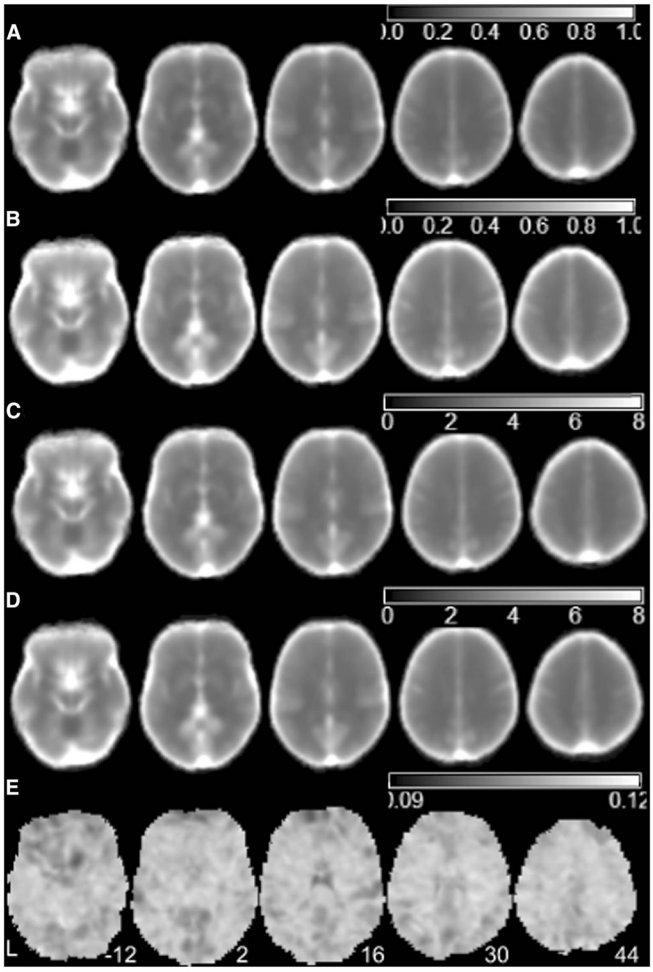

Fig. 1.

Mean nMSSD and VSD maps 16 healthy subjects included in the test–retest dataset. **a**, **b** are the mean nMSSD maps from the scan session 1 and session 2, **c**, **d** are the mean VSD maps from scan session 1 and session 2, respectively, and **e** is the nMSSD/VSD ratio map of a representative subject. *L* the *left* side of the brain. The digital numbers to the *right* of each axial image and the blue lines in the sagittal image indicate the physical locations along z direction (mm) of the corresponding axial images in MNI space

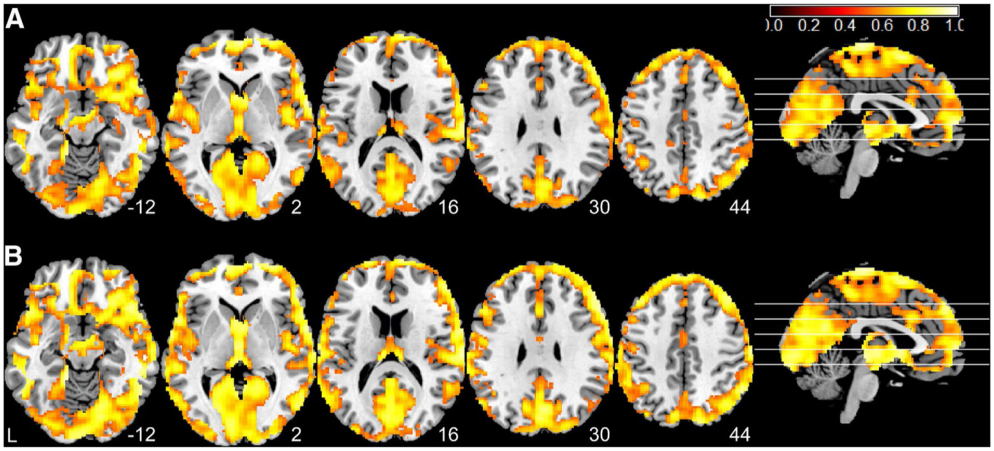

Fig. 2.

Test–retest stability analysis results for **a** nMSSD and **b** VSD. *Hot color* means ICC > 0.5. *L* the *left* side of the brain. The digital numbers to the *right* of each axial image and the *blue lines* in the sagittal image indicate the physical locations along z direction (mm) of the corresponding axial images in MNI space

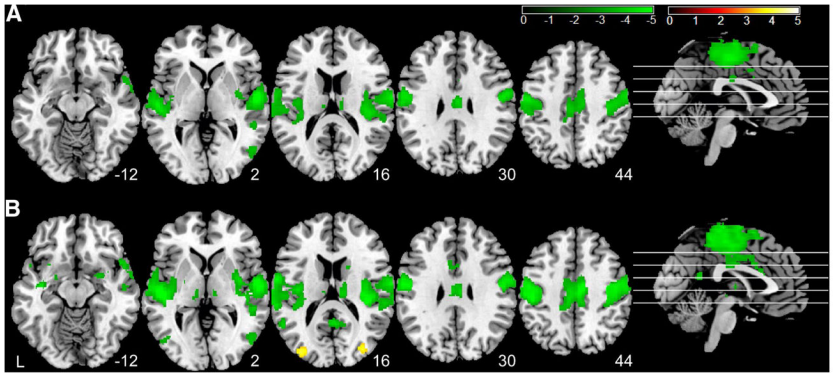

Fig. 3.

Eyes-open versus eyes-closed rsfMRI time-to-time fluctuation difference. **a** Difference of nMSSD and **b** difference of VSD, respectively. Significance level was defined with a voxel-wise $p < 0.001$ (un-corrected) and cluster size >30 voxels. *Hot color* means greater in eyes-open condition; *green color* means greater in eyes-closed condition. *L* the *left* side of the brain. The digital numbers to the *right* of each axial image and the *blue lines* in the sagittal image indicate the physical locations along z direction (mm) of the corresponding axial images in MNI space

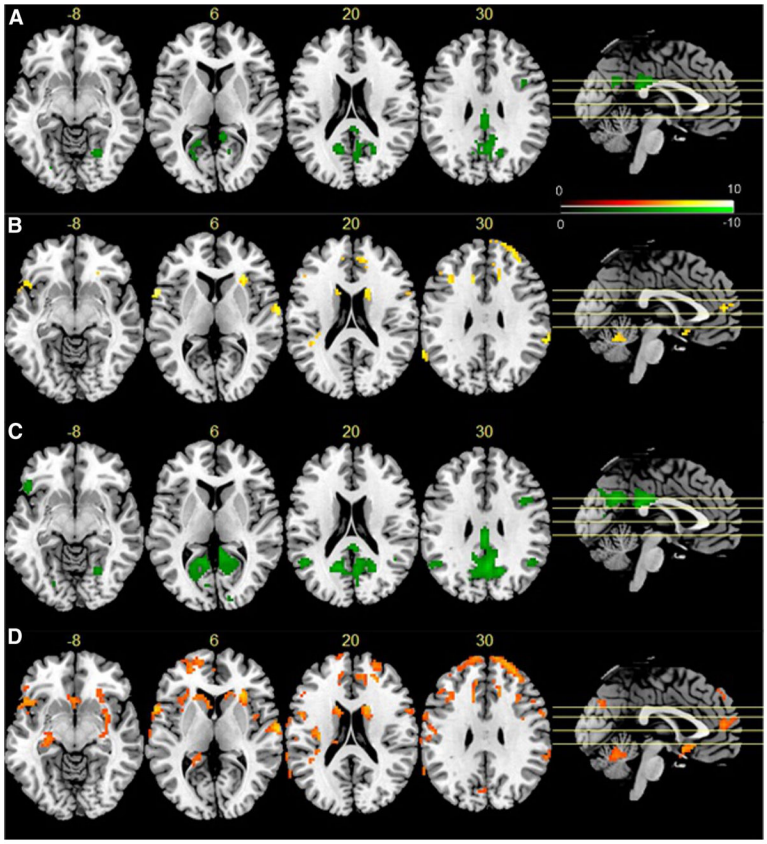

Fig. 4.

Age and gender effects on rsfMRI TTFs. The *green spots* in **a**, **c** indicate negative correlations between age and nMSSD, and VSD, respectively; hot spots in **b**, **d** mean the males had higher nMSSD or VSD, respectively, in those regions. Significance level was defined by $p < 0.05$ (FWE corrected), and cluster size >30 voxels. *L* the *left* side of the brain. The digital numbers to the *right* of each axial image and the *blue lines* in the sagittal image indicate the physical locations along z direction (mm) of the corresponding axial images in MNI space